Research Square

Preprints are preliminary reports that have not undergone peer review.
They should not be considered conclusive, used to inform clinical practice,
or referenced by the media as validated information.

Evolved Gas Analysis and Mechanistic Modeling of Thermal Degradation Products from Polytetrafluoroethylene using Thermogravimetric Analysis- Mass Spectrometry (TGA-MS) and Density Functional Theory

Benjamin R. Johnson
United States Military Academy
Aaron D. Ajeti
Colorado School of Mines
Justin R. Toole
United States Military Academy
Nijel J. Rogers
United States Military Academy
Dairen Jean
United States Military Academy
Taylor N. Miller
United States Military Academy
Jacob R. Nauman
United States Military Academy
Edward L. Zhang
United States Military Academy
Amelia J. Kitlinski
United States Military Academy
Charles M. Aronov
United States Military Academy
Kai D. Palam
United States Military Academy
Andon Z. Thomas
United States Military Academy
H. Daniel Bahaghighat
United States Military Academy
Samuel V. Cowart
United States Military Academy

Corey M. James
United States Military Academy
Pamela L. Sheehan
U.S. Army Combat Capabilities Development Command
Simuck F. Yuk
simuck.yuk@westpoint.edu

United States Military Academy
Shubham Vyas
Colorado School of Mines
Enoch A. Nagelli
United States Military Academy

Article

Keywords: Per- and Polyfluoroalkyl Substances (PFAS), Fluoropolymers, Combustion, Density Functional Theory, Kinetics

Posted Date: August 5th, 2026

DOI: https://doi.org/10.21203/rs.3.rs-10541278/v1

License: This work is licensed under a Creative Commons Attribution 4.0 International License.
Read Full License

Additional Declarations: No competing interests reported.

Evolved Gas Analysis and Mechanistic Modeling of Thermal Degradation Products from Polytetrafluoroethylene using Thermogravimetric Analysis-Mass Spectrometry (TGA-MS) and Density Functional Theory

Benjamin R. Johnson[1,2], Aaron D. Ajeti[3], Justin R. Toole[1], Nijel J. Rogers[1], Dairen Jean[1], Taylor N. Miller[1], Jacob R. Nauman[1], Edward L. Zhang[1], Amelia J. Kitlinski[1], Charles M. Aronov[1], Kai D. Palam[1], Andon Z. Thomas[1], H. Daniel Bahaghighat[1], Samuel V. Cowart[1,2], Corey M. James[1], Pamela L. Sheehan[4], Simuck F. Yuk[1,2], Shubham Vyas[3*], and Enoch A. Nagelli[1,2*]*

[1]Department of Chemical and Biological Science and Engineering, United States Military Academy, West Point, NY 10996, USA; [2]Photonics Research Center, United States Military Academy, West Point, NY 10996, USA; [3]Department of Chemistry, Colorado School of Mines, Golden, CO 80401, USA; [4]U.S. Army Combat Capabilities Development Command, Picatinny Arsenal, NJ 07806, USA.

*Co-corresponding authors: simuck.yuk@westpoint.edu, svyas@mines.edu, enoch.nagelli@westpoint.edu

ABSTRACT

Per- and polyfluoroalkyl substances (PFAS) are a category of compounds whose industrial manufacture can result in environmental contamination that, due to the chemical stability and oleophobic and hydrophobic nature of most PFAS, is challenging to remediate. Fluoropolymers such as polytetrafluoroethylene (PTFE) are a type of PFAS that are not clearly known to be directly toxic, but there is concern that their disposal may lead to subsequent release of more toxic compounds. As such, there is increasing interest in evaluating potential disposal mechanisms, such as incineration, by developing methods to detect and quantify PFAS contamination. In this study, we performed thermal degradation studies on PTFE using thermogravimetric analysis (from 20 to 1000 °C) coupled with mass spectrometry (TGA-MS). Based on the observed TGA-MS experiments conducted on PTFE in open air combustion conditions, a proposed mechanism using a C_{16} molecule, $CF_3(CF_2)_{14}CF_3$, was developed. The kinetic and thermodynamic parameters were evaluated by density functional theory (DFT) and microkinetic models to compare and verify the proposed reaction mechanisms from the experimental TGA-MS data. In addition, process design models were developed using kinetic and thermodynamic reactors before and after the determined gel point for PTFE. The TGA-MS data provides an understanding of the potential gaseous degradation products during the thermal breakdown of PTFE. Ongoing studies aim to investigate potential reaction pathways for degradation of PTFE, other fluoropolymers, and fluoropolymer blends through correlating kinetic and thermodynamic parameters with DFT mechanistic modeling.

Keywords: Per- and Polyfluoroalkyl Substances (PFAS); Fluoropolymers; Combustion; Density Functional Theory; Kinetics

1. INTRODUCTION

Per- and polyfluoroalkyl substances (PFAS) are synthetic, organic chemicals that are one of the most persistent environmental pollutants.[1,2] The designation of synthetic chemicals as PFAS vary as various governmental agencies and researchers provide several definitions. The Environmental Protection Agency (EPA) defines PFAS as chemical substances which contain three distinct structures: R-(CF_2)-CF(R′)R″, where both the CF_2 and CF moieties are saturated carbons, R-CF_2OCF_2-R′, where R and R′ can either be F, O, or saturated carbons, or $CF_3C(CF_3)$R′R″, where R′ and R″ can either be F or saturated carbons.[3] In contrast, the European Chemical Agency (ECHA) defines PFAS as any substance that contains at least one fully fluorinated methyl (CF_3-) or methylene (-CF_2-) carbon atom in the absence of any attached hydrogen, chlorine, bromine, or iodine atoms.[4] The properties of perfluorinated molecules vary greatly based on their structure and the presence of other functional groups. As such, certain perfluorinated compounds vary in their identification as PFAS based on the scope of the respective agency's classification. However, both the EPA and ECHA recognize specific subsets of PFAS as 'forever chemicals' which are harmful to human health and require increased focus on the long-term effects of these compounds, to include perfluorooctanoic acid (PFOA), perfluorooctanesulfonic acid (PFOS), perfluorohexanesulfonic acid, and perfluorononanoic acid.[5] One category of perfluorinated compounds subject to EPA reporting requirements, but not specifically listed as contaminants subject to enforceable limitations, are fluoropolymers, which contain many perfluorinated carbons. The high bond strength of the numerous C–F bonds (the strongest of all organic bonds) makes fluoropolymers very stable and resistant to both thermal and chemical degradation. This resilience has led to worldwide application in a myriad of both industrial and consumer areas including: water-, oil-, and fire-resistant materials;[6] wax coatings on cooking ware; and aqueous fire-fighting foams (AFFFs). There are many widely used fluoropolymers, such as polyvinyl fluoride (PVF), fluoroelastomers, and polyvinylidene fluoride (PVDF). However, the most notable is polytetrafluoroethylene (PTFE), a hydrophobic compound that, at a sufficiently high molecular weight, is inert and insoluble in all known solvents.[7] PTFE

has many global applications including, but not limited to, chemically resistant gaskets, lubricants, pyrotechnics, hydrophobic coatings, and filtration.[8,9]

The high strength of the C–F bond gives give PFAS desirable properties but also make them extremely difficult to break down naturally.[10] As a result, PFAS have accumulated in the environment over the past 70 years.[11,12] This is believed to have contributed to major health and environmental consequences throughout the last century.[13] PFAS contamination is reported to increase the likelihood of contracting certain cancers and decreases the ability of the immune system to respond to infections.[14] PFAS products commonly found in firefighting foams used at both civilian and military airports or hangers have been reported to contaminate the drinking water in surrounding towns and cities, affecting the blood-concentrations of PFAS products in the inhabitants of those surrounding towns.[15]

While the potential toxicity of PTFE is not fully understood, there is concern at the residential scale that PTFE – particularly when used in non-stick cookware and subject to high temperatures – can release toxic chemicals, either from the breakdown of PTFE or the release of other residual chemicals used in an item's manufacture.[16] A similar concern exists at the industrial scale, where incineration is often utilized for disposal of solid waste or PFAS-contaminated soil.[6] There are growing concerns over incineration spreading PFAS contamination, either directly or by decomposing inert fluoropolymers into more harmful byproducts such as EPA-listed PFAS or hydrofluoric acid (HF).[17,18] The first concern is that incineration merely gasifies PFAS, leading to its spread rather than its breakdown.[19] The second concern, the potentially harmful byproducts of PFAS incineration, is more difficult to determine, as many studies into incineration products are in controlled lab settings for a specific PFAS, usually PFOA or PFOS.[18,20] Some studies have established that certain PFAS, such as PTFE, breaks down into HF when incinerated as waste.[21] Another study showed that lower PFAS concentrations in municipal solid waste ash were correlated with an increased incineration temperature, showing that higher temperatures (980 °C) could be more effective at breaking down PFAS.[22]

Several methods have been used to determine characteristics of PFAS and their thermal degradation products, with many different instrumentation techniques utilized.[23–25] Stockenhuber *et al.* used Fourier-transform infrared spectroscopy (FT-IR) and gas chromatography-mass spectroscopy (GC-MS) to analyze the product gasses of PFOA thermal degradation at temperatures as high as 750 °C.[18] Another study on the decomposition of PFOS provided a

theoretical and model-based analysis of the products of the thermal decomposition but did not test the models with any experimental methods.[26] Pyrolysis-gas chromatography-mass spectrometry (py-GC-MS) was used by Lonfei *et al.* to characterize the mechanisms of the pyrolysis of fluoropolymers.[27] This study showed that when the polymer contained monomers with hydrogen such as vinylidene fluoride, the degradation includes the elimination of HF. Krusic and Roe utilized gas-phase nuclear magnetic resonance (NMR) to study the thermal decomposition of ammonium perfluorooctanoate (APFO); while APFO decomposes at a much lower temperature (~350 °C), the method of gas-phase NMR could potentially be used to study other fluorochemicals including PFAS.[28]

In the present study, we performed thermal degradation studies on PTFE using thermogravimetric analysis (TGA), from 20 to 1000 °C, coupled with mass spectrometry (MS). TGA samples using multiple heating rates and gas conditions were analyzed to characterize the evolved gas products and inform potential reaction mechanisms for the decomposition of PTFE in both inert and oxidizing conditions. Based on the observed TGA-MS experiments conducted on PTFE in open air combustion conditions, a proposed mechanism was developed as a reasonable approximation of a long PTFE molecule with a focus on the thermal breakdown steps occurring in the middle of the fragment chain (ignoring the end of the chain). The kinetic and thermodynamic parameters were evaluated by density functional theory (DFT) calculations and DFT-based microkinetic modeling to compare and verify the proposed reaction mechanisms from the experimental TGA-MS data. From the TGA results of thermal PTFE decomposition in open air conditions with a ramp rate of 5 ºC/minute, it was determined that the gel point for the thermal breakdown of the polymer occurred around 550 ºC. Furthermore, the TGA-MS data provides an understanding of the potential gaseous degradation products during the thermal breakdown of PTFE. Understanding the molecular behavior during thermal PTFE degradation also supports insights into the breakdown of other fluoropolymers and blended fluoropolymer materials. Overall, our study provides an integrated perspective on the open-air combustion process of PTFE, linking its molecular-level thermal decomposition mechanisms with macroscopic operating conditions.

2. METHODS

2.1. Experimental Details

Characterization of PTFE samples was carried out using a combination of TGA and MS, as illustrated in **Fig. 1**. TGA was conducted using a TA Instruments TGA55 outfitted with platinum sample pans and an evolved gas furnace with a thermally insulated transfer line, allowing product gases to seamlessly pass to the MS instrument. MS was carried out using an MKS Instruments Cirrus 3 in-line spectrometer with heated stainless steel capillary inlet. The following ion source settings were used for all experiments: emission current 1.00 mA; electron energy 70.00 eV; ion energy 5.0 eV. Most TGA-MS experiments decomposed 12.5 mg of PTFE in the TGA with a gas flow rate of 200 mL/min, consisting of 10 mL/min argon through the balance chamber and furnace (to maintain inert conditions and limit diffusion of product gases) and an additional 190 mL/min of either argon or air directly to the sample furnace. Some preliminary experiments instead used only 10 mL/min of gas direct to the sample furnace (20 mL/min total) to increase MS signal strength and screen for *m*/*z* values of interest. Subsequent runs could focus on that value, which in turn allows the MS to operate with increased sensitivity and scan speed.

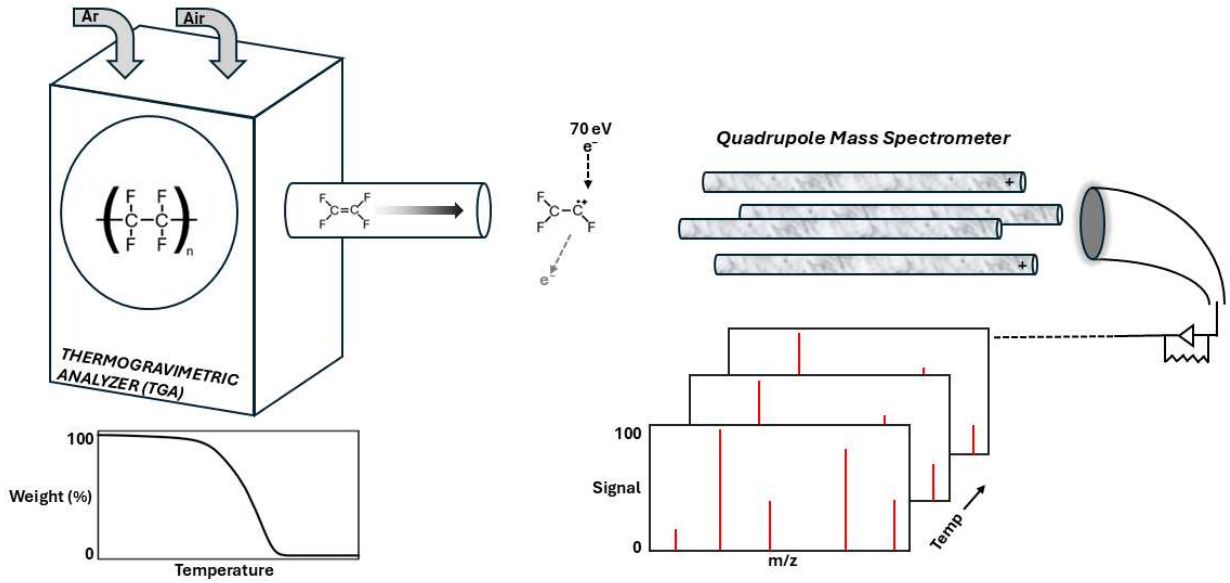


Figure 1: Schematic of experimental procedure.

2.2. Computational Details

All DFT computations were conducted using the Gaussian 16 (Rev. C01)[29] software suite. A perfluoroheptane model was used to explore the bond dissociation energies of various C–C and C–F bonds, while a perfluorohexyl radical was utilized to explore the various downstream

degradation mechanisms. The ground state and transition state structures were optimized utilizing the long-range and dispersion corrected hybrid exchange-correlation functional from Chai and Head-Gordon (commonly referred to as ωB97XD),[30] with triple zeta 6-311+G(d,p) Pople basis sets that include diffuse functions on large atoms and a set of polarization functions on all atoms. It has been shown in the recent past that utilization of ωB97XD density functional yield accurate properties for PFAS and associated reaction pathways.[30] Thermal corrections were performed using Goodvibes software.[31]

Analytical frequencies were obtained to characterize the nature of stationary points. The absence of any imaginary vibrational modes characterized the stationary point as a minimum energy structure, while the presence of one imaginary vibrational mode characterized the stationary point as a transition state structure. Further confirmation of the nature of transition state geometries was performed through intrinsic reaction coordinate calculations.[32] All calculations were performed in the gas phase at standard atmospheric conditions unless otherwise noted.

The DFT-based reaction rate constants were also integrated with a microkinetic model (MKM) for the batch reactor design to study the selectivity and conversion in PTFE degradation mechanisms. Numerical solutions for all ordinary differential equations in the batch reactor models were obtained using a Python script (see Supplemental Information).

3. RESULTS AND DISCUSSIONS

3.1. Kinetic Analysis of TGA Data

Figures 2a and **2b** show the TGA results for decomposition of PTFE at various heating rates (from 2.5 to 20 °C/min) in, respectively, 100% argon and 95% air/5% argon atmospheres. Removing oxygen as a reactant delayed decomposition, such that the maximum rate of decomposition occurred at higher temperatures when reacting in argon compared to air. The difference in temperatures ranged from 12.6 °C (at a heating rate of 2.5 °C/min) to 29.6 °C (at 20 °C/min). This suggests the existence of multiple reactive pathways, with at least one that utilizes oxygen (and is therefore inactive in an inert atmosphere) and at least one that does not.

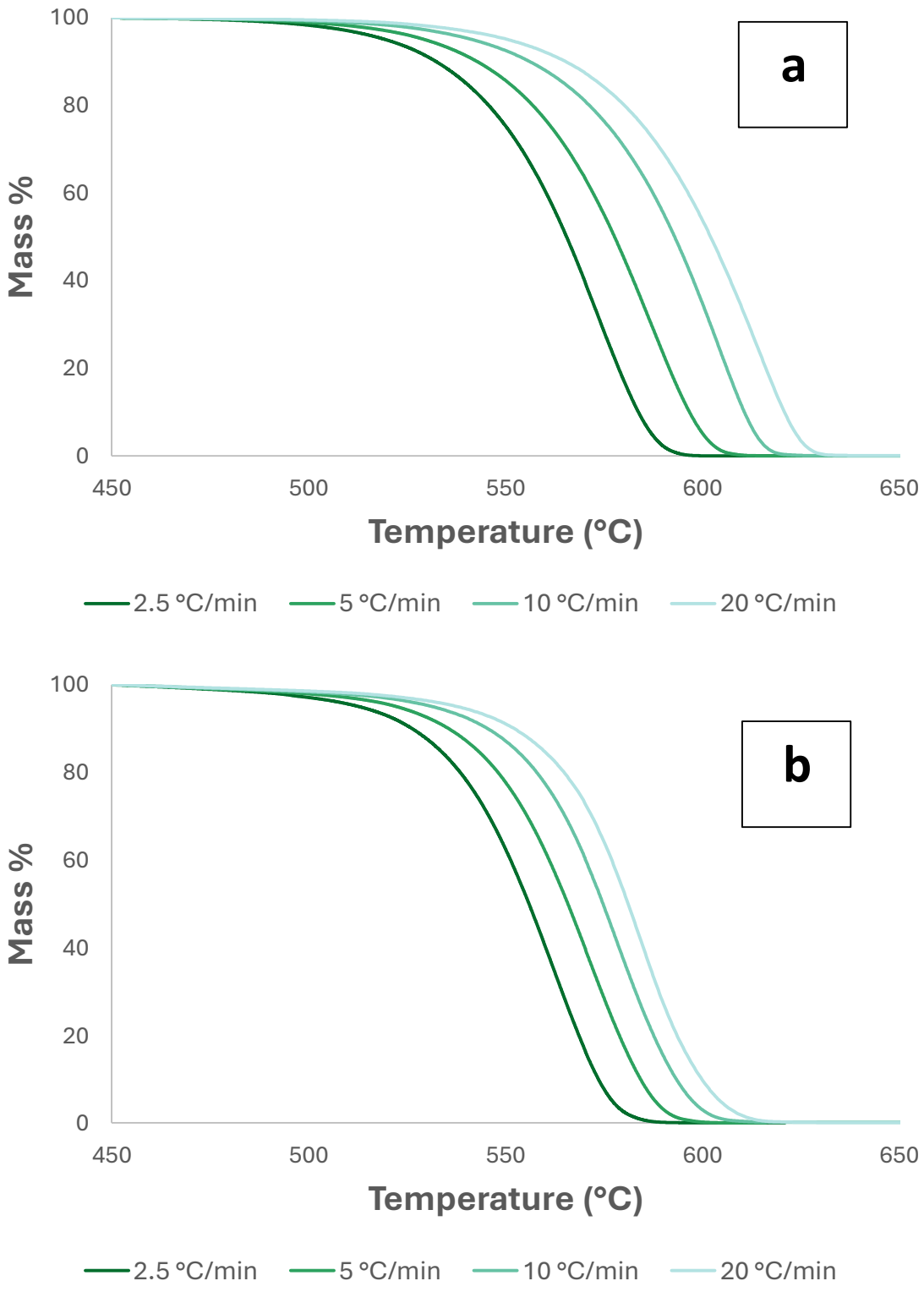


Figure 2: TGA results for PTFE decomposition in a) argon and b) 95% air/5% argon.

Isoconversional analytical methods can be applied to the TGA results obtained at constant heating rates to calculate kinetic parameters such as the activation energy and pre-exponential factor in the Arrhenius equation:

$$\frac{d\alpha}{dT} = \frac{A}{\beta}\exp\left(\frac{-E_a}{RT}\right)(1-\alpha)^n, \quad (1)$$

where α is the fraction of the sample decomposed, T is temperature, E_a is activation energy, A is the pre-exponential factor, β is the heating rate (dT/dt), and n is the order of the reaction. This can be rearranged to

$$\int_0^{\alpha} \frac{1}{(1-\alpha)^n} = g(\alpha) = \frac{A}{\beta}\int_0^{T} \exp\left(\frac{-E_a}{RT}\right) dT, \quad (2)$$

which cannot be solved analytically. The CR method uses an approximation for the right-side integral and rearranges the resulting equation to

$$\ln\frac{\beta}{T^2} = \ln\left[\frac{AR}{E_a g(\alpha)}\left(1-\frac{2RT}{E_a}\right)\right] - \frac{E_a}{R}\left(\frac{1}{T}\right), \quad (3)$$

The apparent E_a for a given α is approximately equal to R times the slope of the line for $\ln\frac{\beta}{T^2}$ vs $\frac{-1}{T}$. The y-intercept of this line can be used to estimate A; this is sometimes simplified by omitting the $\left(1-\frac{2RT}{E_a}\right)$ term, which is close to unity for sufficiently large E_a values.

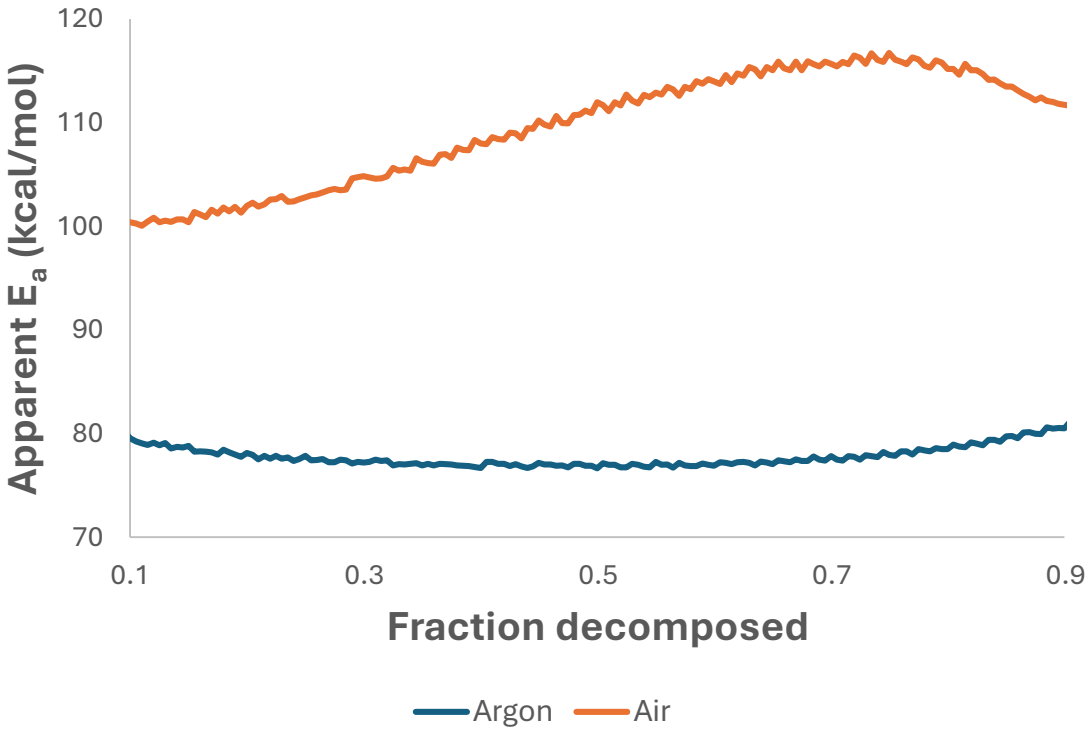


Figure 3: CR analysis of TGA results for PTFE decomposition in argon and air.

Figure 3 shows the results of the CR analysis applied to TGA runs in argon and air for $0.1 < \alpha < 0.9$ (the region for which isoconversional analysis tends to provide stable results). Decomposition in argon shows a relatively constant stable E_a of 77.3 kcal/mol. However, the observed E_a for decomposition in air does not stabilize to a single value. This suggests that decomposition of PTFE proceeds through multiple competing pathways, some of which require oxygen. The selectivity towards these pathways changes with temperature, resulting in a varying E_a when decomposing in air. In the absence of oxygen, some of these pathways deactivate, resulting in a stable E_a. Isoconversional analysis is generally effective for single-step reactions and well-resolved sequential multi-step reactions (where the differential peaks can be deconvoluted), but it is ineffective for resolving simultaneous competing reactions, so no further kinetic information from oxidizing reaction pathways could be obtained from the CR analysis.

3.2. Analysis of MS Data and Product Identification

Figures 4a and **4b** shows the mass spectra of preliminary PTFE samples decomposed in 20 mL/min of either (a) argon or (b) a 50/50 mixture of Ar and air at a constant heating rate of

5 °C/min. MS data was collected for all m/z values up to 300 Da; however, no signals were detected above 150 Da. Based on this data, the main product for PTFE decomposition in inert conditions is the constituent monomer tetrafluoroethylene (C_2F_4; TFE), with characteristic signals at m/z = 31, 50, 81, and 100. Weaker signals at m/z = 69 and 131 indicate that small amounts of larger fluorocarbons, such as hexafluoropropene (C_3F_6; HFP) and C_4F_8 isomers, most likely octofluorocyclobutane based on prior literature.[33,34] A weak signal at m/z = 62 also suggests small amounts of difluoroacetylene (C_2F_2). The strength of these peaks is greatly reduced when decomposing PTFE in air, meaning that less of these fluoropolymer products are made when oxygen is available. Signals at m/z = 47 and 66 indicate that carbonyl difluoride (COF_2) is produced instead, which is consistent with previous studies of PTFE decomposition in oxygen.[25] Additional signals at m/z = 44 (CO_2) and 85–87 (SiF_4) suggest that secondary reactions between product gases and components inside the TGA and/or MS are also occurring.

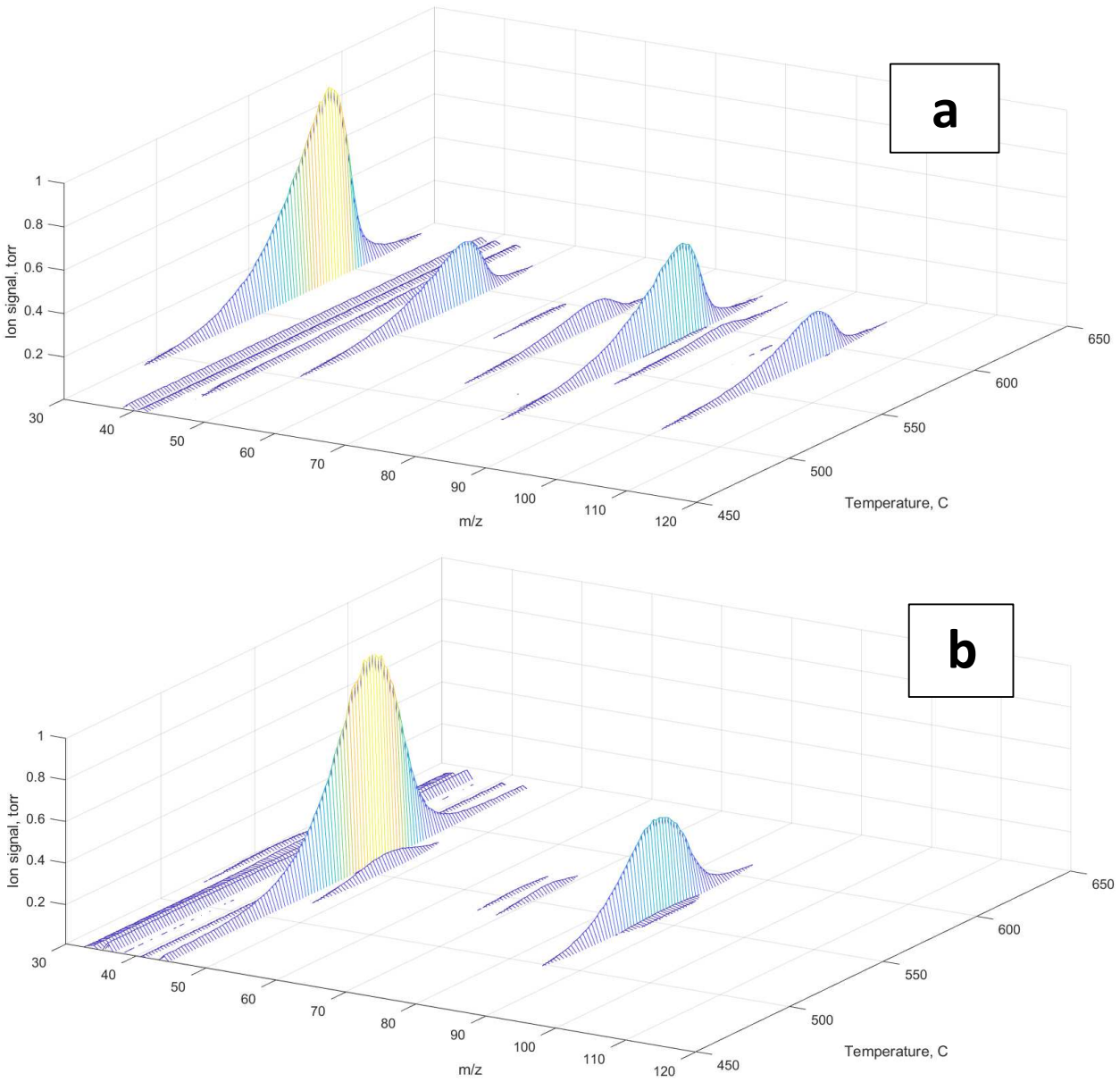


Figure 4: MS results for PTFE decomposition in a) argon and b) 50% air/50% argon.

Table 1: Integrated MS peak signals for select *m*/*z* values for PTFE decomposition in argon and air. Values for each heating rate are normalized to that heating rate's signal for *m*/*z* = 31 in argon.

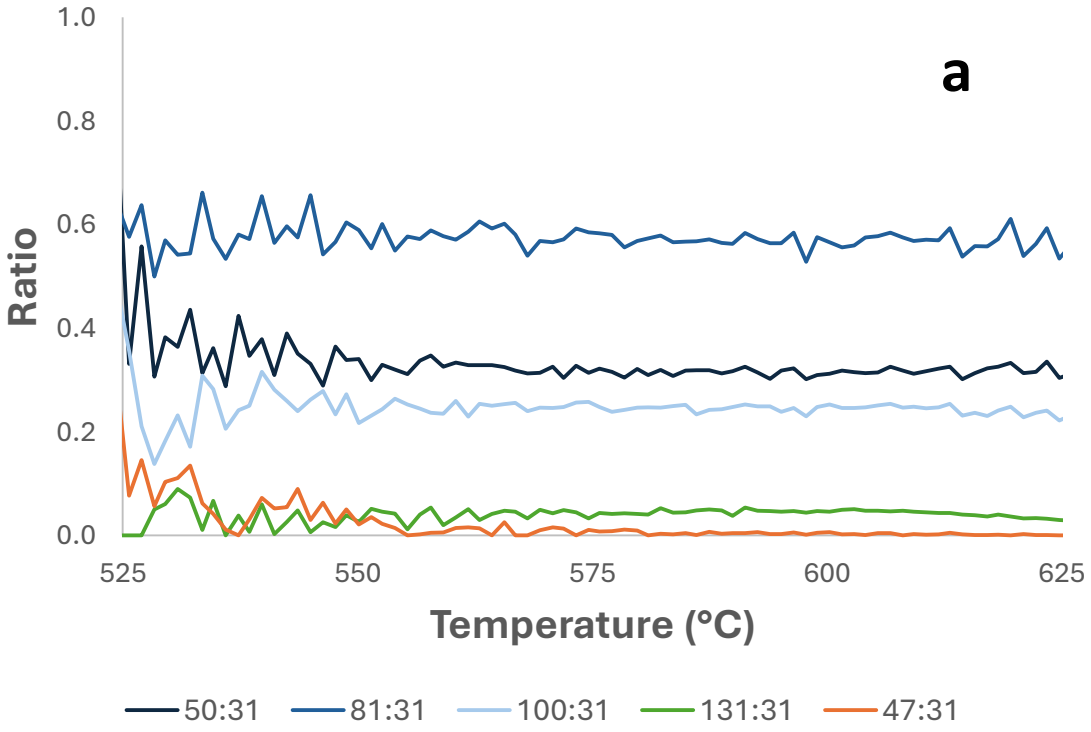
	2.5 °C/min		5 °C/min		10 °C/min		20 °C/min	
m/z	**Argon**	**Air**	**Argon**	**Air**	**Argon**	**Air**	**Argon**	**Air**
31	100.0	35.8	100.0	17.7	100.0	12.1	100.0	14.3
44	5.5	84.2	6.6	66.7	4.7	69.0	4.5	73.8
47	1.3	1.7	0.6	1.9	0.3	9.8	0.4	19.4
50	31.8	3.8	32.2	2.4	31.3	3.2	30.7	3.8
62	0.1	0.7	0.9	0.0	1.0	0.0	0.9	0.0
66	0.0	0.1	0.0	0.0	0.1	2.1	0.0	6.1
69	4.9	1.1	8.7	0.0	8.7	2.3	8.3	3.7
81	55.6	4.1	53.7	4.2	56.3	5.0	54.6	4.3
100	21.0	1.5	22.7	1.4	23.4	1.3	22.9	1.5
131	1.8	0.3	3.4	0.4	3.4	0.3	3.2	0.7
150	0.3	0.0	0.6	0.1	0.6	0.0	0.6	0.0

More accurate MS data can be collected by repeating these experiments while scanning only for the *m/*z values identified in **Fig. 4** as of interest. **Table 1** shows the values of the integrated peak areas collected for these experiments. For each heating rate, the resulting values were normalized so that the peak area for *m*/*z* = 31 in argon is set to 100, making it straightforward to compare the changes associated with the availability of oxygen. The peak areas observed for decomposition in argon are generally consistent with TFE. Introduction of oxygen causes sharp decreases in the signals associated with TFE and the appearance of signals associated with COF_2. These changes become more pronounced (i.e., stronger COF_2 signals and weaker TFE signals) at higher heating rates. This suggests an oxidizing reaction pathway to form COF_2 that is more favorable at high temperatures. At low heating rates, most of the sample decomposes to TFE before this pathway becomes active, while at higher heating rates more sample remains intact when the temperature is high enough for this oxidative pathway to become active.

Figures 5a and **5b** show the results in, respectively, argon and air for the ratios of MS signals for selected *m*/*z* values relative to *m*/*z* = 31, which is the strongest signal observed in TFE. These results were obtained from experiments carried out at a heating rate of 10 °C/min, although the trends observed are the same for all heating rates. In argon (**Fig. 5a**), all ratios are relatively

stable during the period of rapid decomposition, which indicates that decomposition proceeds mainly through a single pathway.

Results for air (**Fig. 5b**), however, have changing values for these ratios. Most notably, the ratio of m/z = 47:31 increases significantly until the temperature reaches roughly 600 °C, the point at which the sample is nearly entirely decomposed. m/z = 47 is the main signal observed in the mass spectrum for COF_2, so this result suggests that the availability of oxygen unlocks a second decomposition pathway that produces COF_2 and is more favorable at higher temperatures.



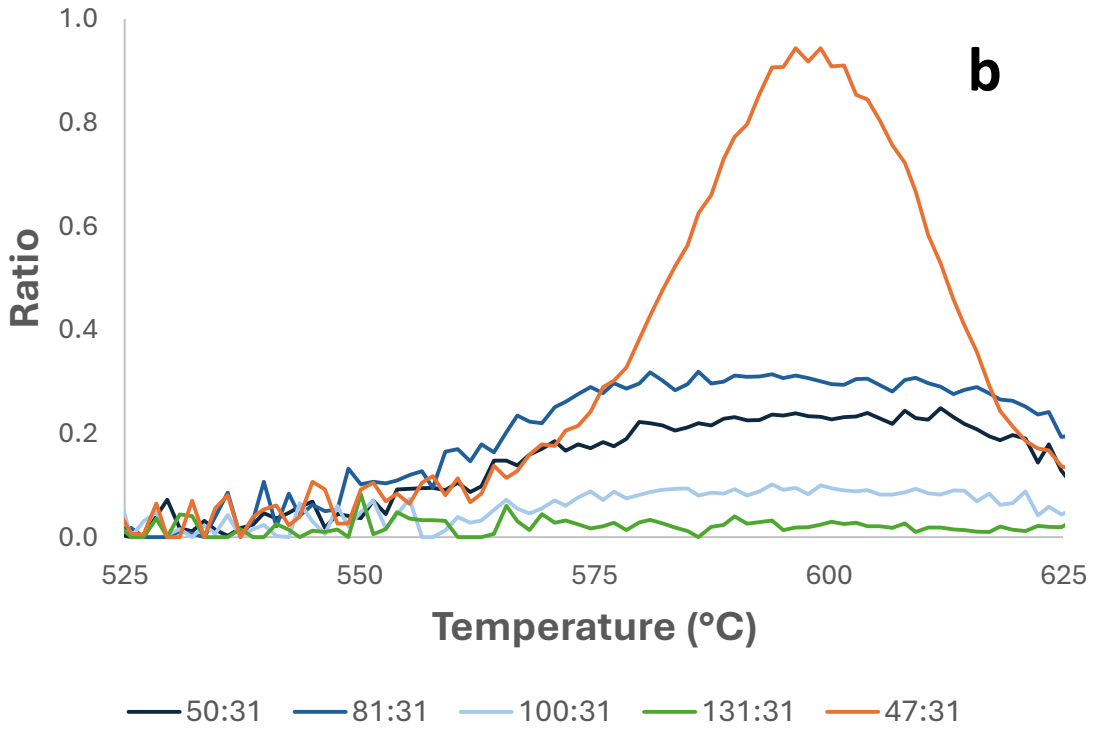


Figure 5: Ratio of select *m*/*z* values during PTFE decomposition in a) argon and b) air.

3.3. DFT-based Mechanistic Pathways of PTFE Degradation

DFT calculations were carried out to model potential reaction steps and pathways for the decomposition/oxidation of PTFE. The entirety of this modeling work is extensive and includes hydrolysis pathways that require substantial concentrations of water or hydrogen (see additional details on DFT-based reaction pathways in Supporting Information). However, discussion here will be limited to three reaction pathways: chain shortening via TFE production, chain shortening via HFP production, and oxidation to COF_2. **Table 2** lists the key reaction steps in these mechanisms along with their corresponding E_a and ΔG values (free energy values are thermally corrected to 795 K). The integers x, y, and z denote arbitrary large numbers typical of long PTFE chains; actual DFT calculations used seven-carbon molecules, which are sufficient to allow for accurate modeling of high-temperature degradation mechanisms while reducing the computational cost of DFT calculations.

Table 2: E_a and ΔG values (in kcal/mol) for steps in selected reaction mechanisms. ΔG values are calculated at 795 K.

Reaction step	E_a	ΔG	G_{start}	G_{TS}	G_{end}
$CF_3(CF_2)_xCF_3 \rightarrow CF_3(CF_2)_y\bullet + CF_3(CF_2)_z\bullet$	78.6	33.9	0.0	78.6	33.9
$CF_3(CF_2)_y\bullet \rightarrow C_2F_4 + CF_3(CF_2)_{y-2}\bullet$	32.4	–4.9	33.9	66.3	29.0
$CF_3(CF_2)_y\bullet \rightarrow CF_3(CF_2)_{y-2}CFCF_3\bullet$	35.8	-9.0	33.9	69.7	24.9
$CF_3(CF_2)_{y-2}C_FCF_3\bullet \rightarrow CF_2CFCF_3 + CF_3(CF_2)_{y-3}\bullet$	29.3	–12.6	24.9	54.2	12.3
$CF_3(CF_2)_y\bullet + O_2 \rightarrow CF_3(CF_2)_yO_2\bullet$	4.1	4.1	33.9	38.0	38.0
$CF_3(CF_2)_yO_2\bullet \rightarrow CF_3(CF_2)_yO\bullet + O\bullet$	55.4	30.1	38.0	93.4	68.1
$CF_3(CF_2)_yO\bullet \rightarrow COF_2 + CF_3(CF_2)_{y-1}\bullet$	2.3	–50.3	68.1	70.4	17.8

Figure 6 illustrates the relative energies of reactants proceeding through these pathways. All mechanisms are initiated through homolytic cleavage of a PTFE chain into perfluoroalkyl radicals, with an E_a of 78.6 kcal/mol and ΔG of 33.9 kcal/mol. Chain shortening via β-scission occurs through a reaction path containing a distinct transition state barrier (E_a = 32.4 kcal/mol; ΔG = –4.9 kcal/mol), which differentiates itself from typical homolytic cleavage where there is no distinct barrier. This effectively results a TFE subunit and a perfluoroalkyl radical fragment. In a previous ReaxFF molecular dynamics study involving pyrolysis of PTFE, TFE formation was observed to be the dominant degradation process at all simulated temperatures, with the major products being C_2F_4, C_2F_6, and C_3F_6.[35] A recent kinetic study on PTFE pyrolysis using DFT calculations also indicated that the initial decomposition primarily occurs through C–C bond scission in unimolecular reactions and hydrogen abstraction in bimolecular reactions, subsequently producing CF_2CF_2 and CF_3CF_2, and eventually leading to CF_3 and CF_2 via β scission and F-migration reactions.[36]

Chain shortening via HFP production is similar but requires an additional step in which an F atom is shifted to the terminal carbon (E_a = 35.8 kcal/mol; ΔG = –9.0 kcal/mol) before cleaving the appropriate C–C bond (E_a = 29.3 kcal/mol; ΔG = –12.6 kcal/mol). The initial cleavage of PTFE into radical fragments can be considered the rate-determining step in both pathways, although TFE formation would then be favored due to the lower activation energy barrier of releasing TFE vs a 1,2–F atom shift.

Oxidation begins with the recombination addition of triple O_2 to the end of a perfluoroalkyl radical fragment to form a perfluoroperoxy radical, $CF_3(CF_2)_yO_2$•, which occurs without a distinct transition state barrier ($E_a = \Delta G = 4.1$ kcal/mol). This is followed by the cleavage of the O–O bond to form a perfluoroalkoxy radical, $CF_3(CF_2)_yO$•, and a monoatomic oxygen ($E_a = 55.4$ kcal/mol; $\Delta G = 30.1$ kcal/mol). This homolytic dissociation reaction process also occurs without a well-defined transition state complex. Additionally, the monoatomic oxygen intermediate is assumed to be short-lived and would be easily abstracted by any surrounding gas-phase radical or reactive oxygen species. Such production of perfluoroalkoxy radicals has also been reported in a TiO_2-based photocatalytic process in the presence of O_2 for the degradation of PFOA.[37] Finally, COF_2 is released through α-cleavage ($E_a = 2.3$ kcal/mol; $\Delta G = -50.3$ kcal/mol). This step contains a distinct transition state structure, which is unlike the reaction steps for oxygen attachment but similar to the β-scission reaction for C_2F_4 or C_3F_6 fragments. The effective activation energy for this process, i.e., the energy difference between the highest-energy transition state in the pathway and the initial reactant, is 93.4 kcal/mol.

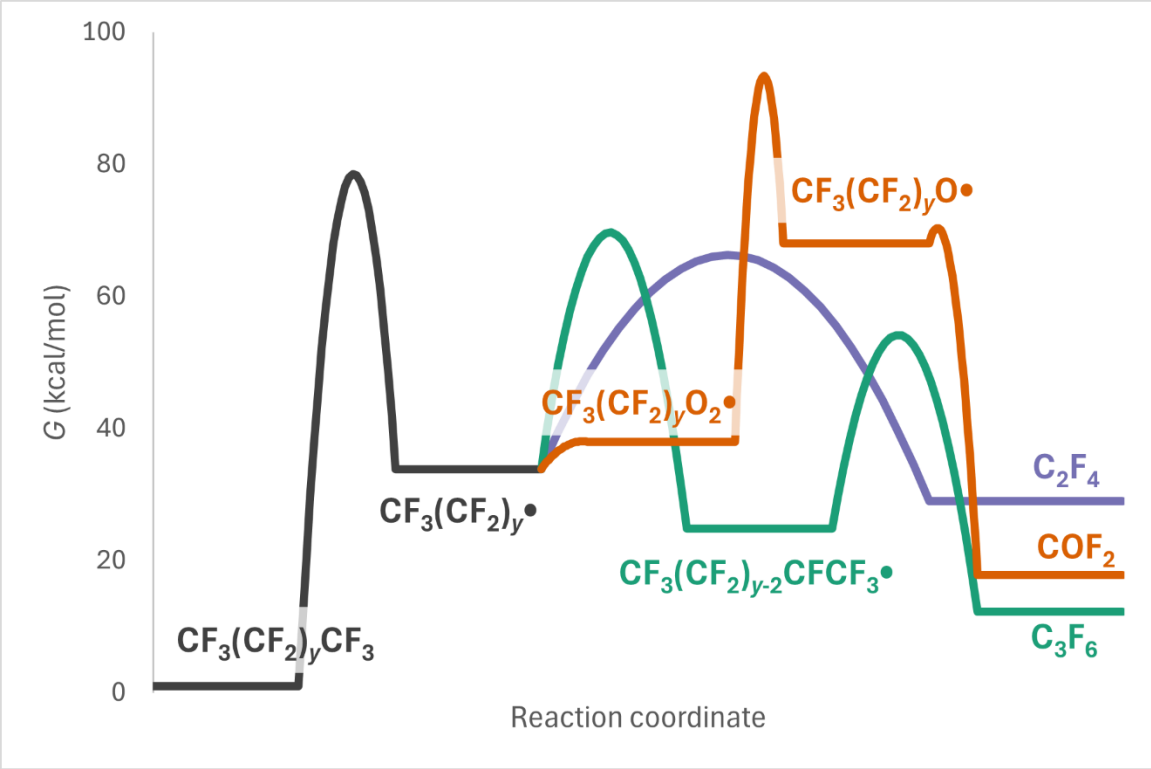


Figure 6: Energy diagram for selected decomposition pathways for PTFE decomposition based on DT calculations of E_a and ΔG at 795 K.

These DFT-based provide an alternative approach to explaining some of the previously inconclusive TGA-MS observations for PTFE decomposition in oxygen A microkinetic model was developed using the mechanism steps, activation energies, and free energy changes obtained from DFT. Simulated TGA runs at different heating rates were carried out using the model and compared to actual TGA data. Several adjustments were made to the mechanism implemented in the MKM to obtain results (**Fig. 7**) that more closely resemble experimental data, leading to potential additional insights on how PTFE might decompose. Specifically, it suggests that the initial step of separating two carbon atoms does not result in completely separated perfluoroalkyl radicals but rather an activated complex that can deactivate before or after release of TFE or other products: $CF_3(CF_2)_xCF_3 \rightleftharpoons CF_3(CF_2)_y\text{-}*\text{-}(CF_2)_zCF_3$. This makes some intuitive sense, a broken C–C bond still leaves two large fluoroalkyl radical segments that cannot move quickly away from each other. If the radicals are treated as completely non-interacting after scission, the equilibrium concentration of radicals (governed by the general equilibrium equation $A \rightleftharpoons 2B$, rather than $A \rightleftharpoons B$) becomes large, and the repetitive nature of TFE release (i.e., a radical can undergo repeated TFE release steps without any additional steps or intermediates) results in PTFE samples decomposing significantly faster in the MKM than observed in TGA experiments. The MKM also suggests that oxygen can react with intact PTFE chains; limiting the oxygenation step to broken or activated C–C bond sites results in models that decompose much slower than TGA experiments indicate. Such a model would feature both oxygenation and TFE pathways using the same active C–C bond intermediate and increasing the rate of COF_2 production restricts the supply of these intermediates and slows TFE generation.

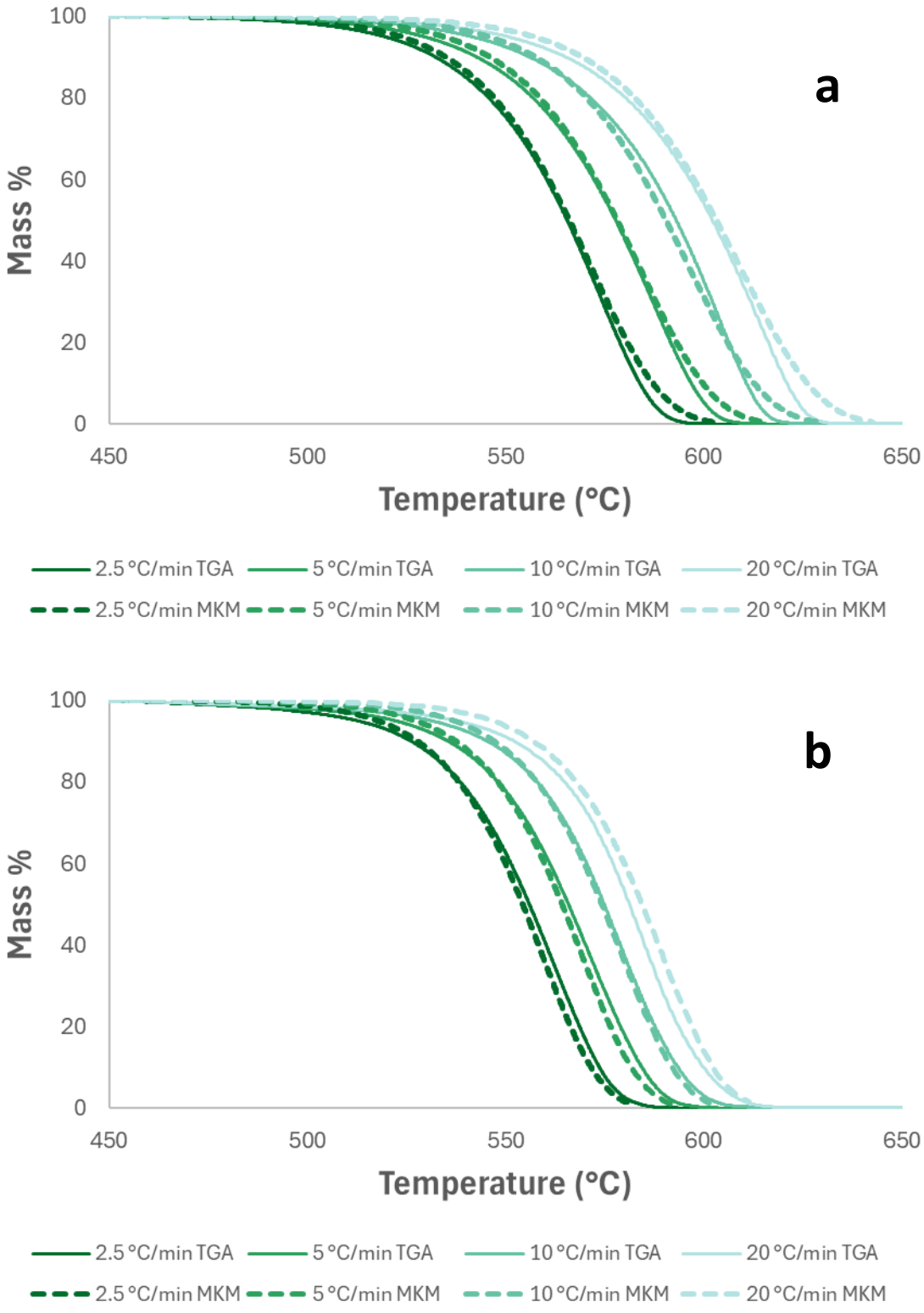


Figure 7: Comparison of MKM results to TGA data for PTFE decomposition in (a) argon and (b) air.

4. CONCLUSION

This study provides an improved understanding of detailed PTFE thermal decomposition mechanisms through an integrated approach combining experimental and computational approaches. Experimental results provide macro-scale data on the kinetics (via TGA) and products (via MS) of PTFE decomposition, while DFT calculations and microkinetic modeling provide a molecular-scale approach to the same system. This demonstrates the value of hybrid experimental/computational research, where experimental results can help direct computational efforts while computations can provide information that is impractical to obtain through experimental means.

Results indicate three likely pathways for PTFE decomposition. First, it can break into constituent TFE monomers. Second, it can break into larger fluorocarbons such as HFP, although this requires additional steps for migrating F atoms along the carbon chain. Finally, it can partially oxidize to COF_2. The only other products observed were very low amounts of difluoroacetylene and C_4F_8 isomers; no larger fluorocarbons or regulated PFAS molecules were detected. HF was also not detected; this is unsurprising given the scarcity of hydrogen in these experiments (only available from trace amounts of water vapor in feed gases), but it is reassuring that HF formation is not particularly aggressive during PTFE decomposition without a more convenient hydrogen source.

Kinetic data such as activation energies and pre-exponential factors were used to develop a MKM that gave a reasonable replication of actual TGA data, although this ultimately required reconsidering some elements of the proposed model. Specifically, the MKM suggests the presence of an activated C–C bond, rather than complete scission into non-interacting fluoroalkyl radicals, and the possibility of oxygen reacting with intact PTFE. While the agreement between experimental and model results suggests that DFT-derived activation energies are reasonably accurate, further study may be required to better understand the transition states involved in this mechanism. Additionally, development of a MKM provides a possible framework examining the yield of decomposition products and how it might be altered through tuning decomposition conditions such as the temperature and ambient gas concentrations. The methods demonstrated here can also be applied to different materials, including both pure materials (e.g., polyvinylidene difluoride, polychlorotrifluoroethylene) and blended/cross-linked materials (e.g., Viton). By

understanding what products are generated from thermal breakdown of these polymers, environmental PFAS contamination might be reduced through better design of processes for thermal disposal and selection of fluoropolymers with preferable thermal decomposition characteristics.

SUPPORTING INFORMATION

Table S1: Complete network of possible PTFE reaction steps analyzed using DFT. **Table S2:** Microkinetic model Python script.

AUTHOR INFORMATION

Corresponding Authors

Simuck F. Yuk: 0000-0003-1355-4400

Shubham Vyas: 0000-0002-5849-8919

Enoch A. Nagelli: 0000-0003-2629-3174

Authors

Benjamin R. Johnson: 0009-0005-9631-3726

Justin R. Toole: 0000-0002-8620-5941

Samuel V. Cowart: 0000-0003-4025-4913

Corey M. James: 0000-0002-5460-7516

Conflicts of Interest

The authors declare no conflict of interest. The funders had no role in the design of the study; in the collection, analyses, or interpretation of the data; in the writing of the manuscript; or in the decision to publish the results.

ACKNOWLEDGEMENTS

This work was financially supported by the Strategic Environmental Research and Development Program (SERDP). Authors also acknowledge allocated computational resources by high performance computing facilities at Colorado School of Mines. The views expressed herein are those of the authors and do not reflect the position of the United States Military Academy, the Department of the Army, or the Department of Defense.

DATA AVAILABILITY

Data will be made available on request.

REFERENCES

(1) Bolan, N.; Sarkar, B.; Yan, Y.; Li, Q.; Wijesekara, H.; Kannan, K.; Tsang, D. C.; Schauerte, M.; Bosch, J.; Noll, H. Remediation of Poly-and Perfluoroalkyl Substances (PFAS) Contaminated Soils–to Mobilize or to Immobilize or to Degrade? *J. Hazard. Mater.* **2021**, *401*, 123892. https://doi.org/10.1016/j.jhazmat.2020.123892.

(2) Merino, N.; Qu, Y.; Deeb, R. A.; Hawley, E. L.; Hoffmann, M. R.; Mahendra, S. Degradation and Removal Methods for Perfluoroalkyl and Polyfluoroalkyl Substances in Water. *Environ. Eng. Sci.* **2016**, *33* (9), 615–649. https://doi.org/10.1089/ees.2016.0233.

(3) United States Environmental Protection Agency. *TSCA Section 8(a)(7) Reporting and Recordkeeping Requirements for Perfluoroalkyl and Polyfluoroalkyl Substances*. https://www.epa.gov/assessing-and-managing-chemicals-under-tsca/tsca-section-8a7-reporting-and-recordkeeping.

(4) European Chemicals Agency. *Registry of Restriction Intentions until Outcome: Per- and Polyfluoroalkyl Substances (PFAS)*. https://echa.europa.eu/registry-of-restriction-intentions/-/dislist/details/0b0236e18663449b.

(5) EPA Press Office. *EPA Proposes Designating Certain PFAS Chemicals as Hazardous Substances Under Superfund to Protect People's Health*. https://www.epa.gov/newsreleases/epa-proposes-designating-certain-pfas-chemicals-hazardous-substances-under-superfund.

(6) Kucharzyk, K. H.; Darlington, R.; Benotti, M.; Deeb, R.; Hawley, E. Novel Treatment Technologies for PFAS Compounds: A Critical Review. *J. Environ. Manage.* **2017**, *204*, 757–764. https://doi.org/10.1016/j.jenvman.2017.08.016.

(7) Puts, G. J.; Crouse, P.; Ameduri, B. M. Polytetrafluoroethylene: Synthesis and Characterization of the Original Extreme Polymer. *Chem. Rev.* **2019**, *119* (3), 1763–1805. https://doi.org/10.1021/acs.chemrev.8b00458.

(8) Dhanumalayan, E.; Joshi, G. M. Performance Properties and Applications of Polytetrafluoroethylene (PTFE)—a Review. *Adv. Compos. Hybrid Mater.* **2018**, *1*, 247–268. https://doi.org/10.1007/s42114-018-0023-8.

(9) Feng, S.; Zhong, Z.; Wang, Y.; Xing, W.; Drioli, E. Progress and Perspectives in PTFE Membrane: Preparation, Modification, and Applications. *J. Membr. Sci.* **2018**, *549*, 332–349. https://doi.org/10.1016/j.memsci.2017.12.032.

(10) Reddy, V. P. *Organofluorine Compounds in Biology and Medicine*; Newnes, 2015.

(11) Evich, M. G.; Davis, M. J.; McCord, J. P.; Acrey, B.; Awkerman, J. A.; Knappe, D. R.; Lindstrom, A. B.; Speth, T. F.; Tebes-Stevens, C.; Strynar, M. J. Per-and Polyfluoroalkyl Substances in the Environment. *Science* **2022**, *375* (6580), eabg9065. https://doi.org/10.1126/science.abg9065.

(12) Buck, R. C.; Franklin, J.; Berger, U.; Conder, J. M.; Cousins, I. T.; De Voogt, P.; Jensen, A. A.; Kannan, K.; Mabury, S. A.; van Leeuwen, S. P. Perfluoroalkyl and Polyfluoroalkyl Substances in the Environment: Terminology, Classification, and Origins. *Integr. Environ. Assess. Manag.* **2011**, *7* (4), 513–541. https://doi.org/10.1002/ieam.258.

(13) National Institute of Enivoronmental Health Sciences. *Perfluoroalkyl and Polyfluoroalkyl Substances (PFAS)*. https://www.niehs.nih.gov/health/topics/agents/pfc.

(14) Kielsen, K.; Shamim, Z.; Ryder, L. P.; Nielsen, F.; Grandjean, P.; Budtz-Jørgensen, E.; Heilmann, C. Antibody Response to Booster Vaccination with Tetanus and Diphtheria in Adults Exposed to Perfluorinated Alkylates. *J. Immunotoxicol.* **2016**, *13* (2), 270–273. https://doi.org/10.3109/1547691X.2015.1067259.

(15) Xu, Y.; Nielsen, C.; Li, Y.; Hammarstrand, S.; Andersson, E. M.; Li, H.; Olsson, D. S.; Engström, K.; Pineda, D.; Lindh, C. H. Serum Perfluoroalkyl Substances in Residents Following Long-Term Drinking Water Contamination from Firefighting Foam in Ronneby, Sweden. *Environ. Int.* **2021**, *147*, 106333. https://doi.org/10.1016/j.envint.2020.106333.
(16) Sajid, M.; Ilyas, M. PTFE-Coated Non-Stick Cookware and Toxicity Concerns: A Perspective. *Environ. Sci. Pollut. Res.* **2017**, *24* (30), 23436–23440. https://doi.org/10.1007/s11356-017-0095-y.
(17) Stoiber, T.; Evans, S.; Naidenko, O. V. Disposal of Products and Materials Containing Per- and Polyfluoroalkyl Substances (PFAS): A Cyclical Problem. *Chemosphere* **2020**, *260*, 127659. https://doi.org/10.1016/j.chemosphere.2020.127659.
(18) Stockenhuber, S.; Weber, N.; Dixon, L.; Lucas, J.; Grimison, C.; Bennett, M.; Stockenhuber, M.; Mackie, J.; Kennedy, E. Thermal Degradation of Perfluorooctanoic Acid (PFOA). *16th Int. Conf. Environ. Sci. Technololgy Rhodes Greece* **2019**.
(19) Wang, B.; Yao, Y.; Chen, H.; Chang, S.; Tian, Y.; Sun, H. Per-and Polyfluoroalkyl Substances and the Contribution of Unknown Precursors and Short-Chain (C2–C3) Perfluoroalkyl Carboxylic Acids at Solid Waste Disposal Facilities. *Sci. Total Environ.* **2020**, *705*, 135832. https://doi.org/10.1016/j.scitotenv.2019.135832.
(20) Watanabe, N.; Takata, M.; Takemine, S.; Yamamoto, K. Thermal Mineralization Behavior of PFOA, PFHxA, and PFOS during Reactivation of Granular Activated Carbon (GAC) in Nitrogen Atmosphere. *Environ. Sci. Pollut. Res.* **2018**, *25*, 7200–7205. https://doi.org/10.1007/s11356-015-5353-2.
(21) Aleksandrov, K.; Gehrmann, H.-J.; Hauser, M.; Mätzing, H.; Pigeon, D.; Stapf, D.; Wexler, M. Waste Incineration of Polytetrafluoroethylene (PTFE) to Evaluate Potential Formation of per-and Poly-Fluorinated Alkyl Substances (PFAS) in Flue Gas. *Chemosphere* **2019**, *226*, 898–906. https://doi.org/10.1016/j.chemosphere.2019.03.191.
(22) Solo-Gabriele, H. M.; Jones, A. S.; Lindstrom, A. B.; Lang, J. R. Waste Type, Incineration, and Aeration Are Associated with per-and Polyfluoroalkyl Levels in Landfill Leachates. *Waste Manag.* **2020**, *107*, 191–200. https://doi.org/10.1016/j.wasman.2020.03.034.
(23) Kupel, R. E.; Nolan, Melvin.; Keenan, R. G.; Hite, Mark.; School, L. D. Mass Spectrometric Identification of Decomposition Products of Polytetrafluoroethylene and Polyfluoroethylenepropylene. *Anal. Chem.* **1964**, *36* (2), 386–389. https://doi.org/10.1021/ac60208a044.
(24) Morisaki, S. Simultaneous Thermogravimetry-Mass Spectrometry and Pyrolysis—Gas Chromatography of Fluorocarbon Polymers. *Thermochim. Acta* **1978**, *25* (2), 171–183. https://doi.org/10.1016/0040-6031(78)85005-9.
(25) Conesa, J. A.; Font, R. Polytetrafluoroethylene Decomposition in Air and Nitrogen. *Polym. Eng. Sci.* **2001**, *41* (12), 2137–2147. https://doi.org/10.1002/pen.10908.
(26) Khan, M. Y.; So, S.; da Silva, G. Decomposition Kinetics of Perfluorinated Sulfonic Acids. *Chemosphere* **2020**, *238*, 124615. https://doi.org/10.1016/j.chemosphere.2019.124615.
(27) Lonfei, J.; Jingling, W.; Shuman, X. Mechanisms of Pyrolysis of Fluoropolymers. *J. Anal. Appl. Pyrolysis* **1986**, *10* (2), 99–106.
(28) Krusic, P. J.; Roe, D. C. Gas-Phase NMR Technique for Studying the Thermolysis of Materials: Thermal Decomposition of Ammonium Perfluorooctanoate. *Anal. Chem.* **2004**, *76* (13), 3800–3803. https://doi.org/10.1021/ac049667k.
(29) Frisch, M. J.; Trucks, G. W.; Schlegel, H. B.; Scuseria, G. E.; Robb, M. A.; Cheeseman, J. R.; Scalmani, G.; Barone, V.; Petersson, G. A.; Nakatsuji, H.; Li, X.; Caricato, M.;

Marenich, A. V.; Bloino, J.; Janesko, B. G.; Gomperts, R.; Mennucci, B.; Hratchian, H. P.; Ortiz, J. V.; Izmaylov, A. F.; Sonnenberg, J. L.; Williams-Young, D.; Ding, F.; Lipparini, F.; Egidi, F.; Goings, J.; Peng, B.; Petrone, A.; Henderson, T.; Ranasinghe, D.; Zakrzewski, V. G.; Gao, J.; Rega, N.; Zheng, G.; Liang, W.; Hada, M.; Ehara, M.; Toyota, K.; Fukuda, R.; Hasegawa, J.; Ishida, M.; Nakajima, T.; Honda, Y.; Kitao, O.; Nakai, H.; Vreven, T.; Throssell, K.; Montgomery, J. A., Jr.; Peralta, J. E.; Ogliaro, F.; Bearpark, M. J.; Heyd, J. J.; Brothers, E. N.; Kudin, K. N.; Staroverov, V. N.; Keith, T. A.; Kobayashi, R.; Normand, J.; Raghavachari, K.; Rendell, A. P.; Burant, J. C.; Iyengar, S. S.; Tomasi, J.; Cossi, M.; Millam, J. M.; Klene, M.; Adamo, C.; Cammi, R.; Ochterski, J. W.; Martin, R. L.; Morokuma, K.; Farkas, O.; Foresman, J. B.; Fox, D. J. Gaussian 16 Revision C.01, 2016.

(30) Hoomissen, D. J. V.; Vyas, S. Early Events in the Reductive Dehalogenation of Linear Perfluoroalkyl Substances. *Environ. Sci. Technol. Lett.* **2019**, *6* (6), 365–371. https://doi.org/10.1021/acs.estlett.9b00116.

(31) Luchini, G.; Alegre-Requena, J. V.; Funes-Ardoiz, I.; Paton, R. S. GoodVibes: Automated Thermochemistry for Heterogeneous Computational Chemistry Data [Version 1; Peer Review: 2 Approved with Reservations]. *F1000Research* **2020**, *9*, 291. https://doi.org/10.12688/f1000research.22758.1.

(32) Fukui, K. The Path of Chemical Reactions - the IRC Approach. *Acc. Chem. Res.* **1981**, *14* (12), 363–368. https://doi.org/10.1021/ar00072a001.

(33) van der Walt, I. J.; Neomagus, H. W. J. P.; Nel, J. T.; Bruinsma, O. S. L.; Crouse, P. L. A Kinetic Expression for the Pyrolytic Decomposition of Polytetrafluoroethylene. *J. Fluor. Chem.* **2008**, *129* (4), 314–318. https://doi.org/10.1016/j.jfluchem.2008.01.003.

(34) Bezuidenhoudt, A.; Sonnendecker, P. W.; Crouse, P. L. Temperature and Pressure Effects on the Product Distribution of PTFE Pyrolysis by Means of Qualitative, in-Line FTIR Analysis. *Polym. Degrad. Stab.* **2017**, *142*, 79–88. https://doi.org/10.1016/j.polymdegradstab.2017.05.025.

(35) Ajeti, A. D.; Vyas, S. Gas Phase Product Evolution during High Temperature Pyrolysis of PTFE: Development of ReaxFF Simulation Protocol. *Chem. Eng. J. Adv.* **2024**, *19*, 100622. https://doi.org/10.1016/j.ceja.2024.100622.

(36) Wang, Y.; Wang, S.; Chu, Q.; Chen, D. Pyrolysis Kinetics of Polytetrafluoroethylene (PTFE). *Int. J. Quantum Chem.* **2025**, *125* (3), e70015. https://doi.org/10.1002/qua.70015.

(37) Sansotera, M.; Persico, F.; Rizzi, V.; Panzeri, W.; Pirola, C.; Bianchi, C. L.; Mele, A.; Navarrini, W. The Effect of Oxygen in the Photocatalytic Oxidation Pathways of Perfluorooctanoic Acid. *2015 ACS Award Issue "For Creat. Work Fluor. Chem. Veronique Gouv.* **2015**, *179*, 159–168. https://doi.org/10.1016/j.jfluchem.2015.06.019.

Supplementary Files

This is a list of supplementary files associated with this preprint. Click to download.

- PTFEThermalDegradationSIFinal.docx